UNIVERSIDADE FEDERAL DE UBERLÂNDIA
FACULDADE DE ENGENHARIA MECÂNICA

FABIO MACHADO ALVES DA FONSECA

ANALYSIS OF TOMOGRAPHIES OF CAVITIES OBSERVED UNDER DECOMPRESSION OF ELASTOMERS EXPOSED TO HYDROGEN

UBERLÂNDIA, MG

2022

FABIO MACHADO ALVES DA FONSECA

ANALYSIS OF TOMOGRAPHIES OF CAVITIES OBSERVED UNDER DECOMPRESSION OF ELASTOMERS EXPOSED TO HYDROGEN

Final work for the graduation, presented to the Aeronautical Engineering Course of the Faculty of Mechanical Engineering, to obtain a bachelor's degree in Aeronautical Engineering.

Supervisors: Dr. Giuliano Gardolinski Venson; Dr. Azdine Nait-Ali; Dr. Sylvie Castagnet

UBERLÂNDIA, MG

2022

Acknowledgements

First of all, I would like to thank my supervisors Mrs Castagnet and Mr Nait-Ali for trusting me toface the subject of this internship and for giving me inspiration, guidance and their blessing to finish it.I also want to thank my family, Fernando, Rosângela and Gabriel, for their prayers and support during this long time without seeing them. Finally, I am grateful for my friends, who helped me a lot in finishing this internship, mainly Marcos Gonçalves, Vinicius Moretto, João Oliveira and Alexis Pelletier.

List of Tables

List of Figures

Contents

1. Introduction

Pprime institute is a big laboratory in the field of Mechanics and Energetics in France. It is headed by CNRS (UPR 3366), École Nationale Supérieure de Mécanique et d'Aérotechnique (ISAE-ENSMA)and the University of Poitiers, converting it in one of the highest names in transport, energy and materials. The institute PPrime is also associated with NANOIMAGESX (Synchrotron SOLEIL). This means that the lab has access to the technology of particle accelerator that will be used in this study.

At the department of Damage and Durability of Pprime Institute, the team has been interested in the formation of cavities in rubber materials exposed to hydrogen under high pressures followed by decompression. The phenomena was observed for the first time in 1990 and has not been widely investigated so far. In the last years, the usability of rubbers in industry has increased regarding its unique properties and benefits of efficiency and cost. In this context, connected to the world's pressure of reducing emissions of greenhouse gases and clean sources of energy usage, we have the perfect environment. It is the opportunity to make this study of cavities one of the heads to encourage transportation moved by hydrogen, showing that we are close to have enough technology to improve the hydrogen volume energy efficiency within a reduced cost.

In this sense, the Pprime institute has recently developed an experience of in-situ monitoring of decompression with tomographies which provides access for the first time to a time-resolved 3D visualization of the field damage. In this way, it was possible to obtain a quantification over time of parameters such as number of cavities, size distribution, their relative distances and their form factor. This experiment, so far carried out on X-ray source of the laboratory, was recently brought to a synchrotron environment in order to gain in space and time resolution. In this sense, the objective of this internship was to contribute to the analysis of tomographies images acquired during the recently conducted test campaign on the Anatomix beamline of the Synchrotron SOLEIL.

During this study, it was possible to observe a lot of new phenomena never noticed before. In this situation, it was necessary to stipulate specific objectives taking into account the duration of the internship. They were: understanding better the formation of cavities with the new resolution in time and space resultant of the Synchrotron SOLEIL, elucidating the mechanisms at a very early stage; capturing new effects such as sphericity, volume of the sample, distance between cavities and the freesurface, and distance between

cavity-cavity. Furthermore, it was possible to work with more severe conditions of decompression to obtain more cavities into the experiment to improve the statistical analysis. Lastly, the influence of the crosslink density with the formation of cavities was analyzed.

The work was carried out on the ImageJ software, on the basis of already existing processing programs that were adapted, particularly to deal with a large number of data. The first step was to specify the mechanisms already demonstrated in an EPDM (Ethylene Propylene Diene Monomer) and to raise some questions about the early stages of growth.

2. Context

2.1 Position of the subject

Around the 70's, big companies started investing in the hydrogen technology. Currently, we have the first cars moved by hydrogen. We are talking about changing a century-old paradigm with a new infrastructure, a hydrogen economy. In this big project, some problems became known. One example is the formation of cavities in the tanks of hydrogen. To have a volumetric efficiency, we need to store hydrogen under high pressures (70 MPa) and due to the act of filling and emptying the tank, there is the formation of cavities that leads to crack initiation on the elastomer components of the tank.

2.2 Suggests literature survey

The first studies around the 90's announced the phenomena of cavities in polymers exposed to high pressure gas and decompressed. A few years later, they focused on finding critical values to the formation of cavities, like a critical pressure of decompression for each polymer. It means that under that pressure they were safe from having cavities and consequently crack initiation.

Nowadays, the hypothesis well accepted for the formation of cavities, in the academic environment,is that during a compression of an Ethylene Propylene Diene Monomer (EPDM) the molecules of hydrogen will enter the material and generate a state of equilibrium. Once started the decompression, these molecules will try to leave the sample, but they will have a problem of instability due to the bifurcation phenomenon. Thanks to this instability, the formation of cavities will happen.

In this sense, experiments needed to be conducted to understand it better. Due to the complexity and danger of the experiment, only two laboratories in the world had enough technology to conduct a decompression with a flammable gas and acquire images at the same time. One of these labs is the Pprime institute. The two following sections will summarize the latest studies of the research group responsible for this subject.

2.2.1 Review "In-situ X-ray computed tomography of decompression failure in a rubber ex-posed to high-pressure gas" [1]

In this study, we had the first time-resolved 3D images of the process that we had the chance to observe the evolution of the volume of the cavities. The methodology of this study was the same of the next study that will be describe with more details. By that time, in result of a bad resolution, the growth kinetics of the cavities was ignored. Then, we observed the distribution of cavities through thethickness, showing that there are more cavities in the heart of the sample. Finally, the anisotropy of the cavities (how much spherical the cavities are) was studied, showing a profile that increases quickly in the beginning of the decompression until anisotropy is equal to one (perfectly spherical) and then decreases along with time.

2.2.2 Review "Local kinetics of cavitation in hydrogen-exposed EPDM using in-situ X-Ray to-mography: focus on free surface effect and cavity interaction" [2]

This study guided the objectives of this internship and was the reference for our results. In this paper, two samples of Ethylene Propylene Diene Monomer (EPDM) were studied, one with a crosslink density of $4{,}21 * 10{-}5$ mol/cm3, so called EPDM 0,5 in the following sections, and the other one with density of $2{,}81 * 10{-}4$ mol/cm3, called EPDM 1,6. In easy words, crosslink density is the amount of connection points between the carbon chains of the elastomer. Thus, the in-situ tomography was conducted in two different decompression conditions: the first one with $P_{sat} = 8\ MPa$ and a pressure release rate of 1,6 *MPa/min*; and the second one with $P_{sat} = 12\ MPa$ and a pressure release rate of 2,5 *MPa/min*.

To better understand the way that the experiment was operated, which is also the same methodology used to acquire the tomographies in the Synchrotron SOLEIL, the Figure 2.1 represents role of pressure over the time, illustrating the P_{sat} and the decompression.

Figure 2.1 - Representation scheme of the experiment.

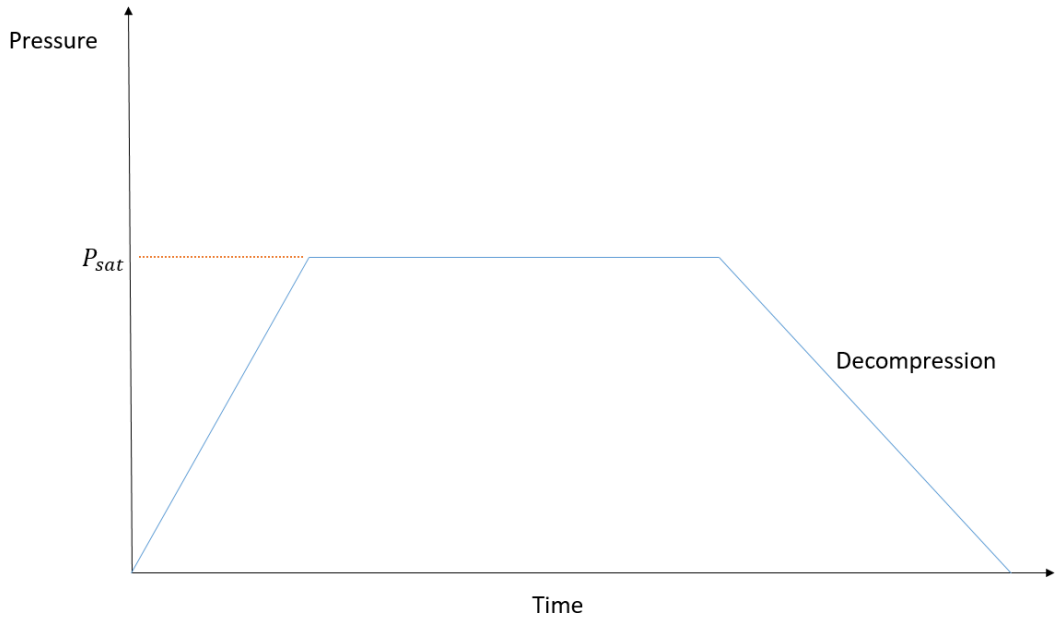

Source: Ownership by author (2022)

A methodology of separating the cavities into three families was applied, based on the morphology of them, and illustrated in Figure 2.2:

- Isolated cavities: cavities without intrusion of other cavities into the processed volume during the whole evolution;
- Close cavities: cavities with intrusion of other cavities into the processed volume during the investigated time;
- Clusters: set of close cavities that were not distinguishable due to the space resolution and were treated like one cavity.

Figure 2.2 - Families of cavities. (a) isolated cavities - (b) close cavities - (c) clusters.

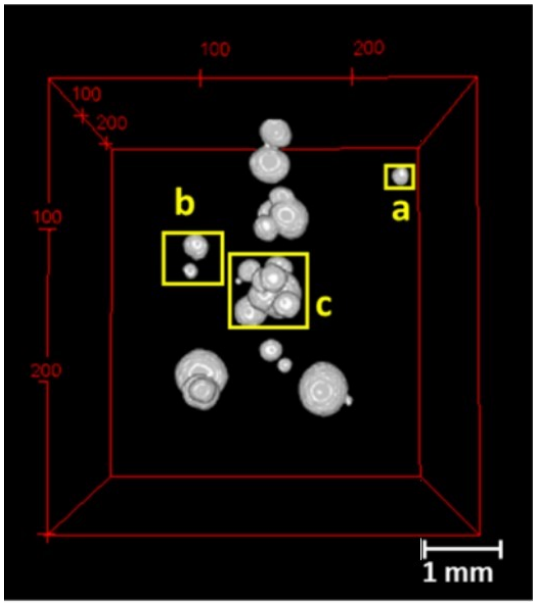

Source: FAZAL, M. et al (2020)

After the division, the inflation characteristics were observed only for the group (a) - isolated cavities and (b) - close cavities, shown in the Figure 2.3.

Figure 2.3 - Volume evolution of groups of cavities.

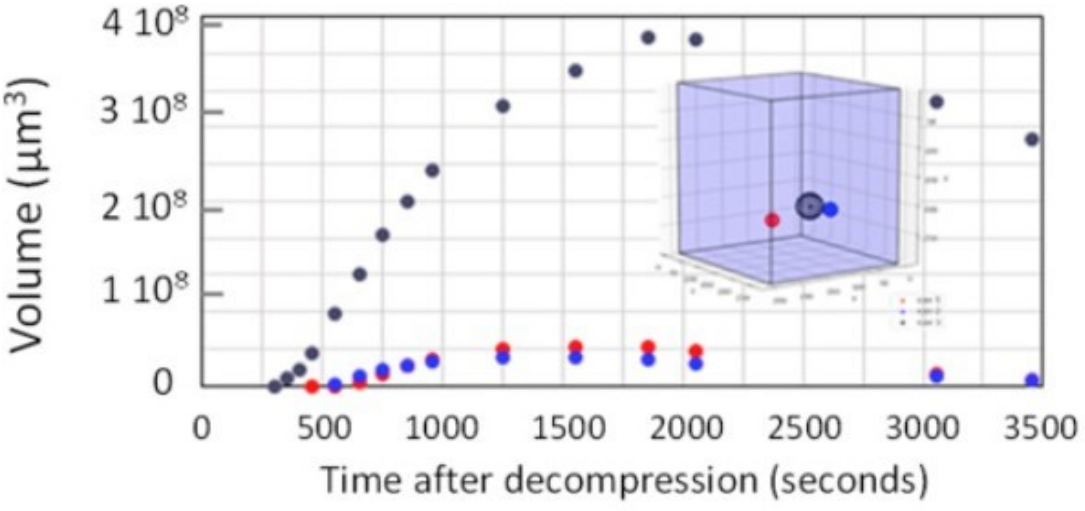

Source: FAZAL, M. et al (2020)

It is visible that the resolution in time and space turns the mechanism of growth into a linear approximation. Along with the brief introduction given in this paper, the objective of the internship was also to focus on the very earliest stages of the process.

3. Methodology

The experiments were conducted in the Anatomix beamline of the Synchrotron SOLEIL with the same methodology of the latest paper and with a rectangular sample of dimensions 2 *mm x* 2 *mm x* 5 *mm*. The goal of the internship was just to treat and analyze the tomographies already acquired. It is important to note that in the previous study we had a space resolution of 16 μm and a time resolution of 100 *s* (time to make one tomography). With the data obtained in Synchrotron SOLEIL, the space resolution jumped down to 3 μm and time resolution to 4 *s*. Associated with the better resolution, it comes the memory problem. Each tomography needs 3,125 *Gb* of space and each sample showed in the Table 3.1 has 121 tomographies totaling 378,125 *Gb* for one sample and 3,025 *To* for the whole data without treatment.

Table 3.1 - Data acquired separated by crosslink density.

Crosslink density	Sample	P_{sat} [MPa]	Pressure release rate [bar/min]
EDPM 1,6	ECH 14 - decompression 47	12	25
	ECH 14 - decompression 49	12	25
	ECH 18 - decompression 72	12	120
	ECH 15 - decompression 52	12	120
EDPM 0,5	ECH 17 - decompression 68	12	120
	ECH 19 - decompression 73	12	120
EDPM 0,1	ECH 16 - decompression 63	12	120
	ECH 20 - decompression 75	12	120
	ECH 13 - decompression 45	12	120

Source: Ownership by author (2022)

To treat the tomographies, a harsh treatment method was developed, creating a standard process toavoid errors and to make it possible to compare the samples. It is important to notice that the crosslinkdensity of the EPDM 1,6 and 0,5 are the same of the study already described, and the EPDM 0,1 has adensity of $1,96 * 10^{-3}\ mol/cm^3$.

3.1 Image processing

The image processing of the tomographies was done using a plug-in of ImageJ®, the Fiji. This powerful tool was able to pick the tomographies in *.vol* (this is a simple file, consisting of a header and a set of value bytes, for storing volume image data) and open it as *RAW* (file not yet processed and therefore it is not ready to be used) in Fiji. One tomography is divided in 800 images, each image with the size of 1000 x 1000 pixels, illustrated in the Figure 3.1.

Figure 3.1 - Representation of one tomography.

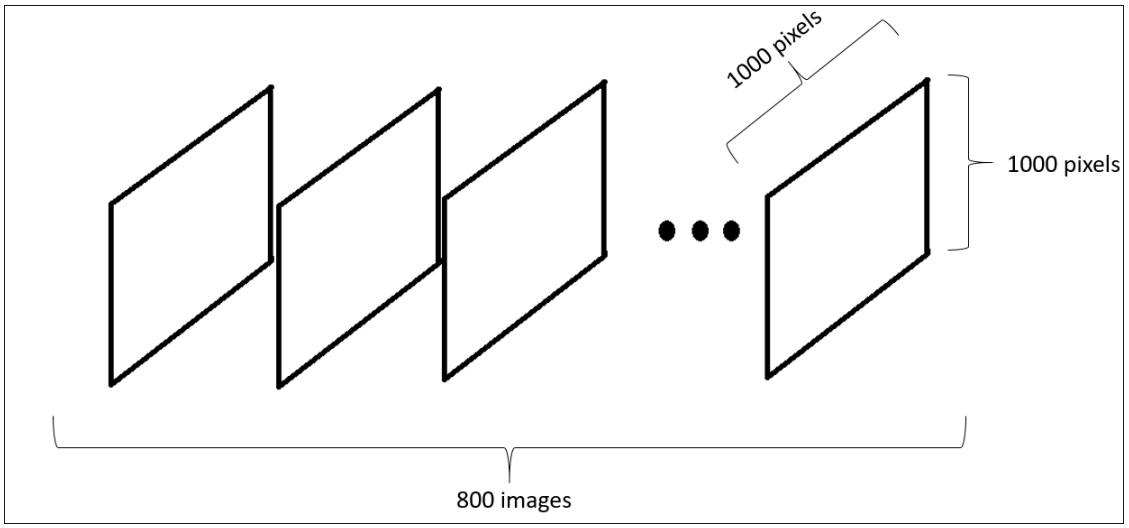

Source: Ownership by author (2022)

With all the tools of Fiji, an automatic process was created with a Macro to treat each one of the 800 images and later save them in *.tiff* (Tag Image File Format - flexible and adaptable file format for handling images and data within a single file, storing image data in a lossless format). Figure 3.2 shows all this process of treatment. The objective of this procedure was to highlight the cavities and the free edge, removing the noises. Moreover, it is important to note that the steps showed in the Figure 3.2 were found by testing the tools of Fiji until having the noises eliminated.

Figure 3.2 - Flow chart of the Macro

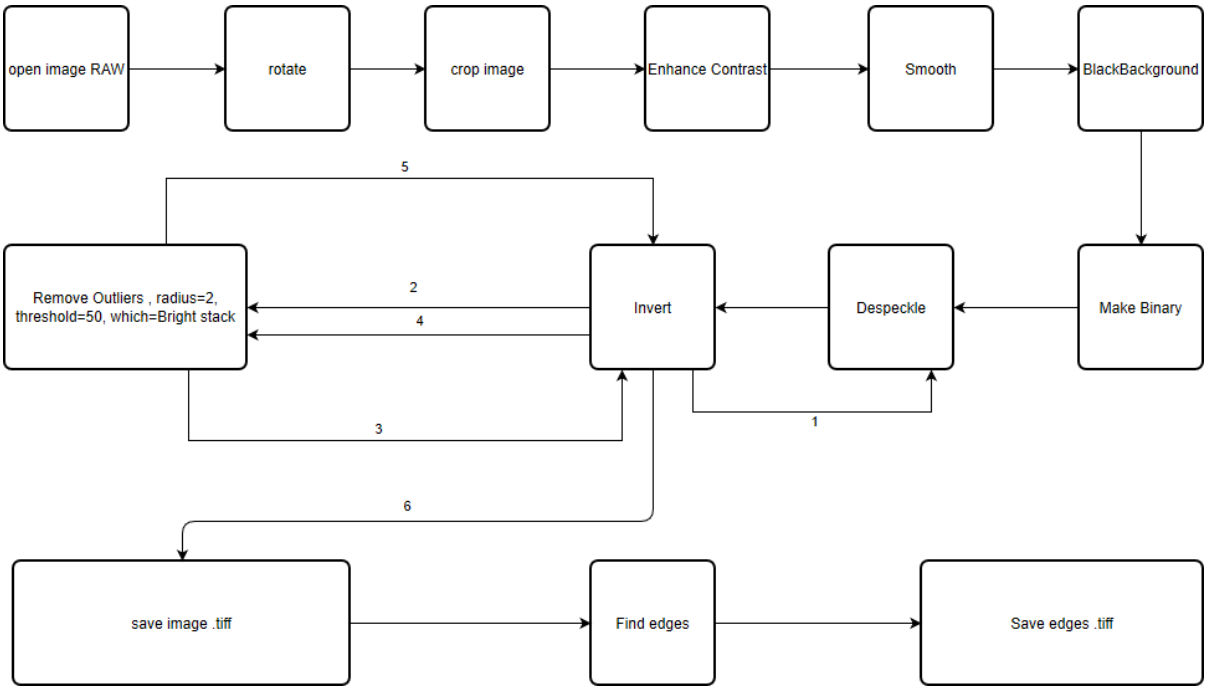

Source: Ownership by author (2022)

Figure 3.3 shows the tomography before treatment (first block of the flow chart) and the binary image already treated (three last blocks of the flow chart).

Figure 3.3 - Example of the image *RAW* compared to the image already treated also with the edges.

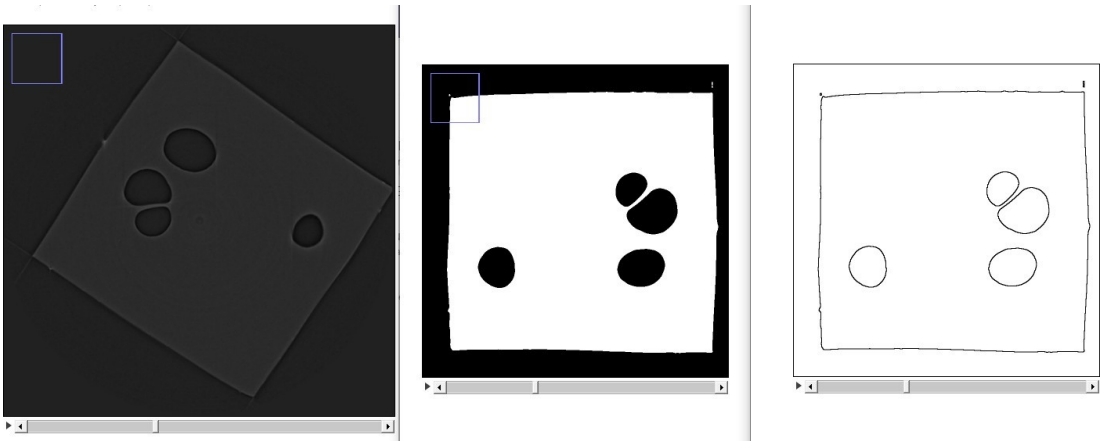

Source: Ownership by author (2022)

With the image in the format *.tiff*, it was possible to extract the properties of the sample with a Matlab script.

3.2 Determination of the properties with Matlab®

With the binary image, we created a 3D matrix that would be the input for the function **region-props3**. This function can determine some cavity's properties like:

- 'Centroid' - Center of mass of the region, returned as a 1-by-3 vector of the form [$centroid_x$ $centroid_y$ $centroid_z$]. The first element, $centroid_x$, is the horizontal coordinate (or x-coordinate) of the center of mass. The second element, $centroid_y$, is the vertical coordinate (or y-coordinate).The third element, $centroid_z$, is the planar coordinate (or z-coordinate). Basically, the Matlab script creates a matrix with the indexes of each voxel (cubic element with size 1 pixel x 1 pixel x1 pixel) and then calculates the coordinates mean within the three directions to find the centroidof the cavity;

- 'Volume' - Count of the actual number of 'on' voxels in the region, returned as a scalar. Volume represents the metric or measurement of the number of voxels in each region within the volumetric binary image. In order to calculate the volume, the Matlab script picks the same matrix of indexes, representing the voxels, and makes a simple sum to determine the volume, given in voxels;

- 'Principal Axis Length' - Length (in voxels) of the major axis of the ellipsoid that has the same normalized second central moments as the region, returned as 1-by-3 vector. The determination of the ellipsoid with the same normalized second moments is a complex process already validated for Matlab. In easy words, the second central moment is the covariance matrix instead of the variance, because the cavities are three-dimensional. Basically, the Matlab code fits a multivariate normal distribution to the cavities. The covariance matrix determines the distribution's shape and the contour lines of a multivariate normal distribution are overlapped, giving an ellipsoid.

- 'Eigenvalues' - Eigenvalues of the voxels representing a region, returned as a 3-by-1 vector. regionprops3 uses the eigenvalues to calculate the principal axes lengths;

- ’Eigenvectors’ - Eigenvectors of the voxels representing a region, returned as a 3-by-3 vector. regionprops3 uses the eigenvectors to calculate the orientation of the principal axes lengths of the ellipsoid that has the same normalized second central moments as the region;

Furthermore, with the biggest and the smallest principal axes lengths, a new property was definedand named sphericity (named anisotropy in the latest studies), meaning how much spherical the cavitywas. It is given by the equation (1).

$$\text{Sph} = \frac{\text{Principal axis}_{max}}{\text{Principal axis}_{min}} \quad (1)$$

Moreover, to determine other properties such as distance cavity-cavity, distance free surface - cavity and volume sample, a black-box code (property of the institute PPrime) was used. Furthermore, the biggest challenge was to make the relation between the labels (cavities) over the time. Indeed, each tomography had a quantity of labels that could change the numeration over time.

Figure 3.4 - Change of labels over the time.

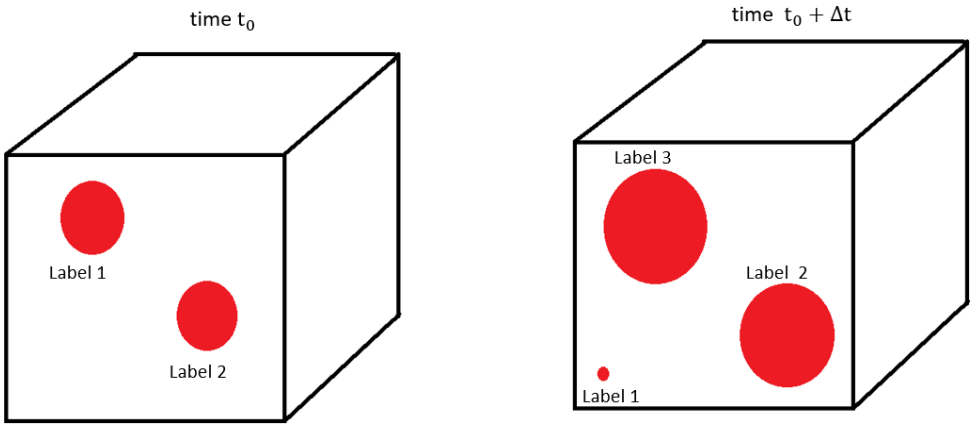

Source: Ownership by author (2022)

Figure 3.4 illustrates the problem "by default": Label 1 at time t0 is the Label 3 of time t0 +Δt and Label 1 at time t0 +Δt is a new cavity. To fix this problem, it was necessary to create a code to make a correlation of labels over the time. The logic used to create the code was to look at the variation of the centroid between two tomographies and pick the

smallest distance. For example, if we pick the coordinates(x,y,z) of the centroid of the Label 1 at t_0 and calculate the Euclidean distance to all the labels at the time t0 + Δt, we will have the smallest distance with the Label 3. This means that the cavity 1(notation) at the tomography t0 has a label of 1 and at the tomography t0 +Δt has a label of 3. These information was saved in a matrix named **mat-ind-lab**.

At this point, we have all the elements to start the analysis of the properties. Figure 3.5 shows the flow chart of all the process in Matlab®.

Figure 3.5 - Flow chart of the process to determine and analyze properties. In red, the black-box code and in green the codes developed during the internship.

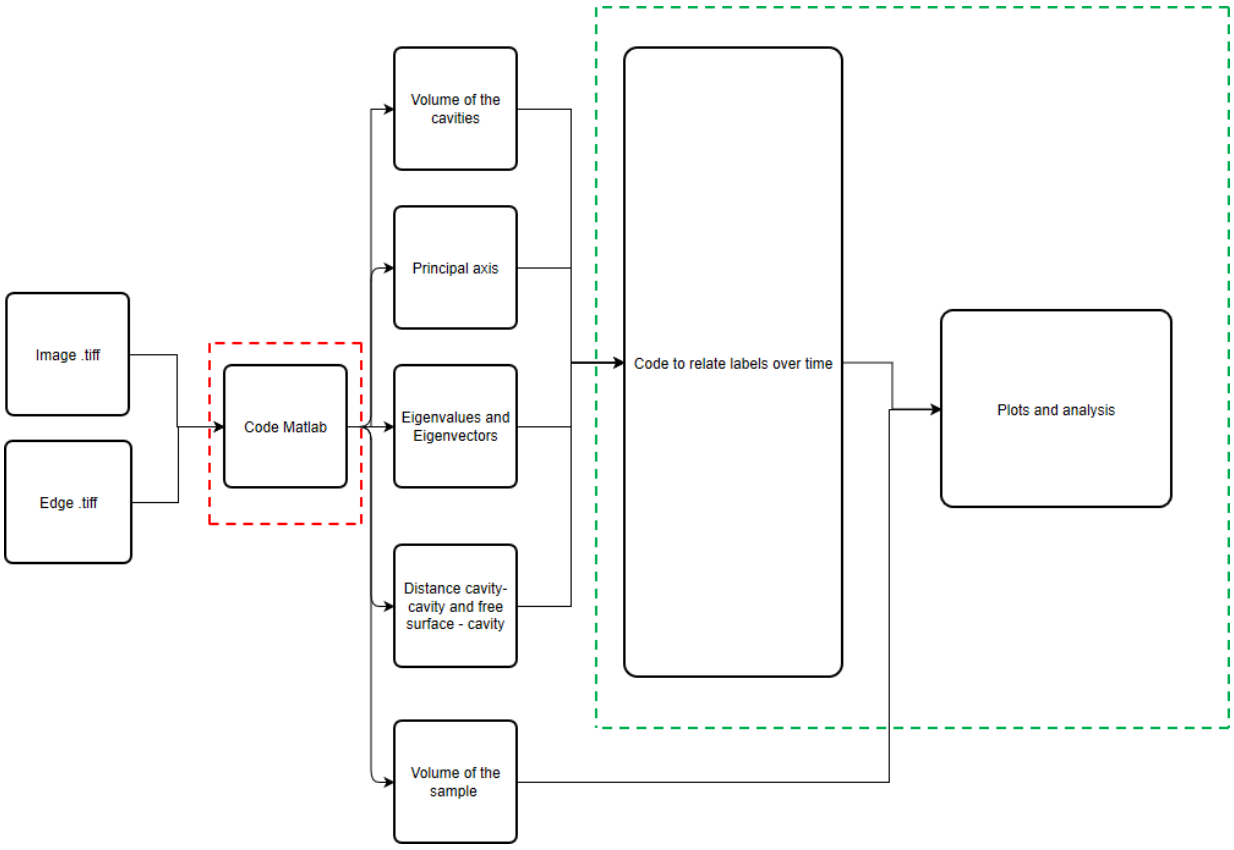

Source: Ownership by author (2022)

3.2.1 Codes for plots and analysis

All the plots shown in the next section were made by a code developed during the internship. Moreover, during the internship, two types of analysis were created:

- Interpolation to have the coefficients of the graph volume vs time for each cavity;

- Evolution of the principal axis and its direction over time.

3.3 3D visualisation

The 3D visualization was very important to validate the results, understand better the phenomena and look at the details of the sample and cavities. In the beginning, following the methodology of the latest studies, ParaView was used to validate the labels over the time with a 3D visualization. Nevertheless, with the space and time resolutions, the software demanded 140 *Gb* of RAM memory(4 times more than available) to display the content. Therefore, an alternative way was created, doinga code in Matlab to display cavities in the space, using a tool of 3D viewer in Fiji and a tool of Windows®, named Visionneuse 3D. With this package, we were able to validate the results and look the phenomenon in detail. Figure 3.6 illustrates the example of the new package for the 3D visualization.

Figure 3.6 - Example of 3D validation with the new package.

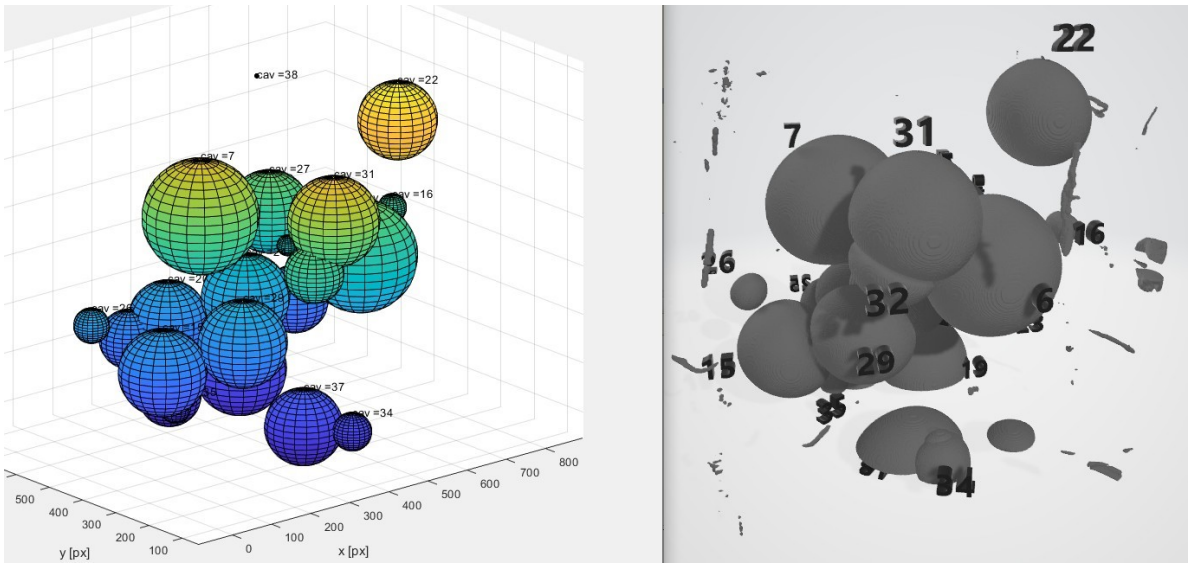

Source: Ownership by author (2022)

4. Results and discussion

At this point, we have all the elements to begin the data analysis. In order to have a logical and understandable order, this section was split in four topics: the study of growth mechanisms, the effect of close cavities, the damage mechanisms and the effect of cavities on global inflation of the sample.

The EPDM 1,6 was the first being tested during the campaign. The first pressure release rate applied was 25 bar/min, but only one cavity was observed in the sample ECH 14-47 (ECH 14 - decompression47) and none in the ECH 14-49. Thus, it was decided to increase the pressure release rate to 120 bar/min for all the following tests.

4.1 Growth mechanisms of isolated cavities

According to Fazal et al. (2020), cavities without intrusion of other cavities into the processed volumeduring the whole evolution are named isolated cavities. Analyzing some of these cavities, a typical profile was observed for the volume evolution over time, summarized in Figure 4.1 and Figure 4.2. First, the cavities grow respecting a parabola opening to the top, named inflate curve in this study. Then, they pass for a inflection point and start to follow a new parabola opening to the bottom, named deflate curve, until the volume is stable to a constant value. It is important to state that it was very hard to find isolated cavities in this study. Due to the small size of the sample tested, the cavities were always under edge effects [2] or the effect of close cavities. Even with this restriction, when found, they respected the profile.

Figure 4.1 - Typical profile of isolated cavities.

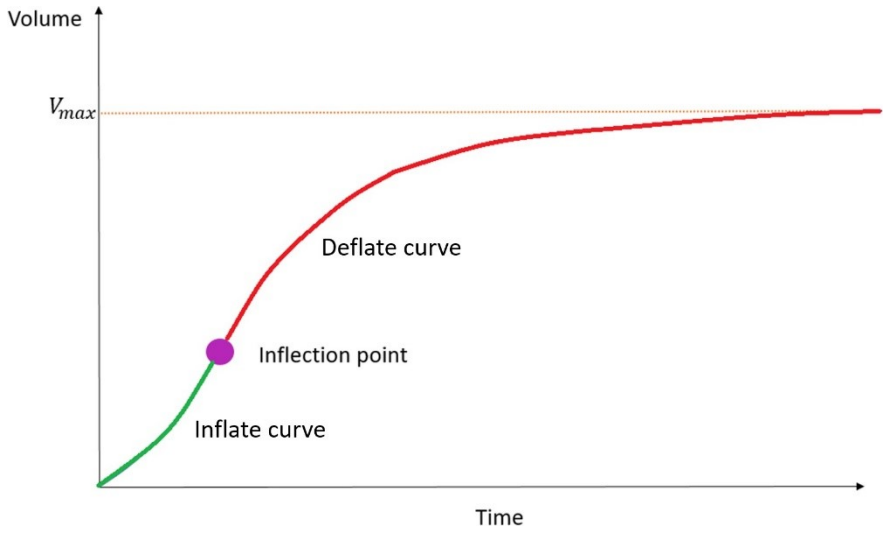

Source: Ownership by author (2022)

It is important to note that these two regimes were identified for the very first time in this study. They were not accessible in the previous works due to time and space resolutions. In the last studies, the growth mechanism of isolated cavities was about a straight line (Figure 2.3), lacking information regarding the growth kinetics.

As shown in section **3.2.1 - Codes for plots and analysis**, a code was created to make a polynomial interpolation beginning at the first apparition of the cavity until the inflection point (green curve - Figure 4.1) and a second interpolation beginning at the inflection point until the point of maximum volume (red curve - Figure 4.1). A second degree polynomial was chosen to fit both curves, because a parabola could greatly describe each of them. Further, the constant value of the second derivative of the interpolation function represents the growth's acceleration of a cavity. The methodology used for the interpolation can be found in section 6.

Subsequently, those coefficients were compared and, as a result, a linear correlation between the inflate and the deflate acceleration was found, meaning that the way the cavity inflates determines theway that it deflates. Also, with these results, the approach of a linear growth for the cavities is a good approximation and the rate coefficient (slope) can represent the phenomena. Therefore, the approach of the latest work was validated.

Figure 4.2 – On top, the 3D image with the labels of the tomography 100 (t = 400 s) for the ECH 17 - 68 and at the bottom, the evolution of the volume and sphericity over time for isolated cavities (6 and7).

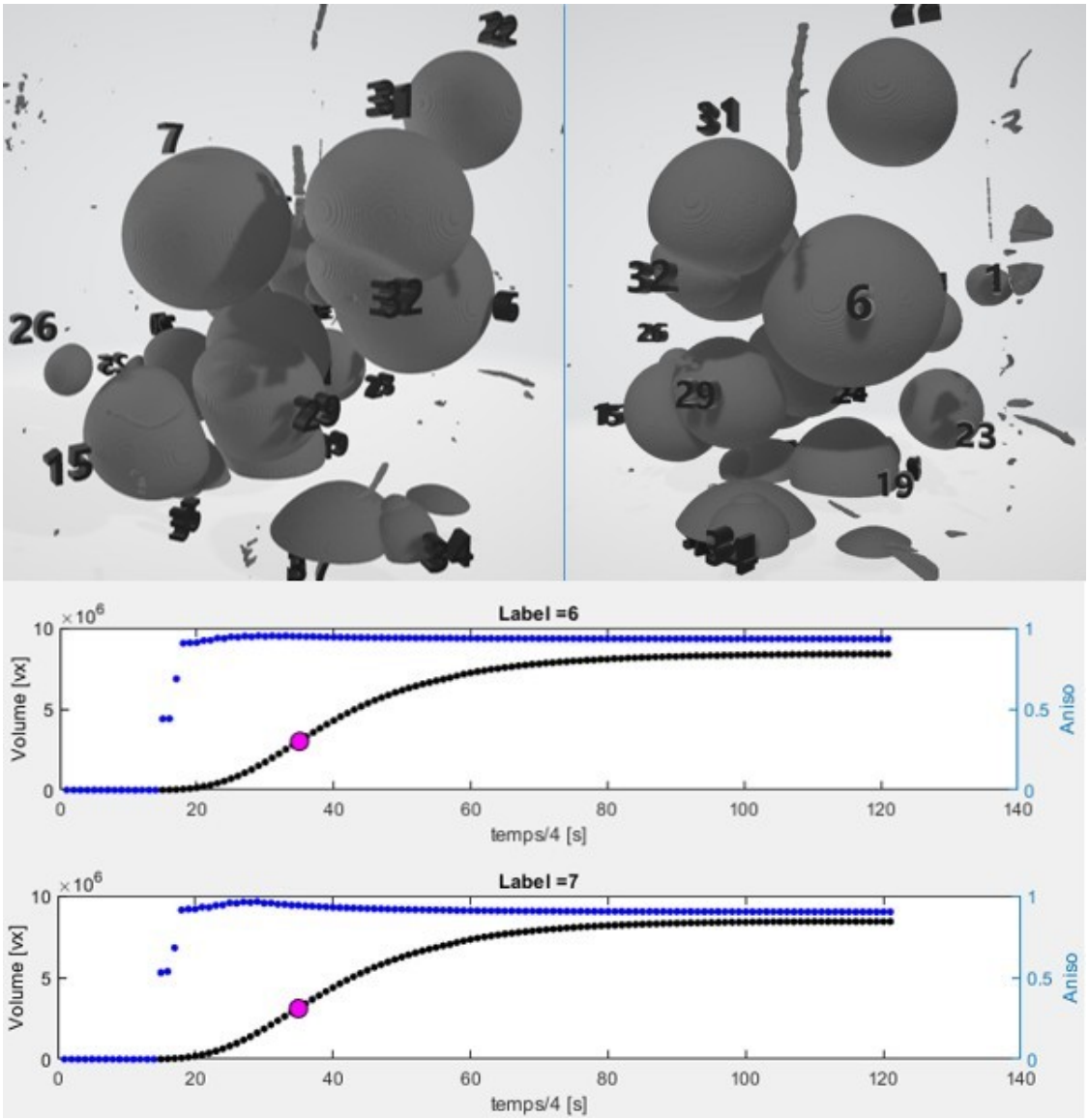

Source: Ownership by author (2022)

Furthermore, this analysis was not made only for isolated cavities, but for all cavities on the sample, yielding at the same trend. It suggests that the linear correlation does not depend of the conditions around the cavity, actually it is an intrinsic phenomenon of it, as shown in the Figure 4.3.

Figure 4.3 – The abscissa represents the inflation rate $\left[\frac{vx}{s^2}\right]$ and the ordinate represents the absolute value of the deflation rate $\left[\frac{vx}{s^2}\right]$ for EPDM 1.6

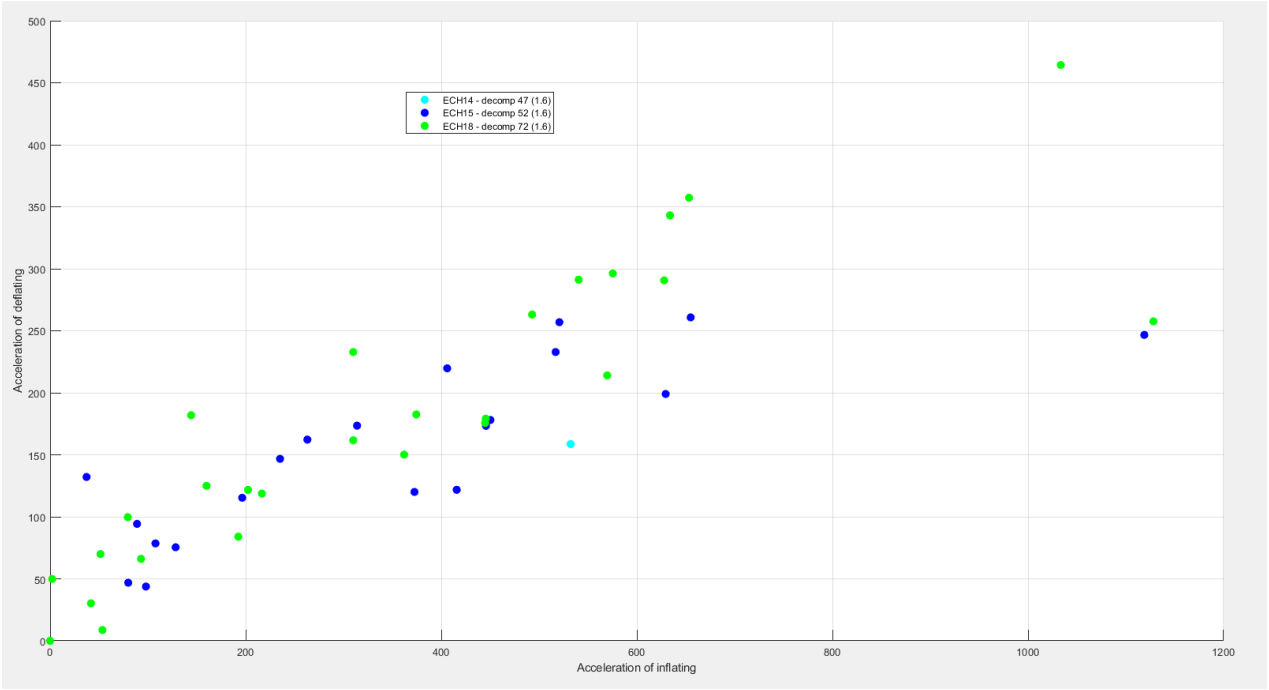

Source: Ownership by author (2022)

Likewise, it was observed that isolated cavities have the biggest accelerating coefficients. A hypothesis was made taken into account the observations in the study of Castagnet et al. (2018), where it was evidenced that more cavities were nucleated in the heart of the sample. In this sense, it suggests that cavities far enough from the free surface have a different environment to grow and it could have an influence in the accelerations of the cavities. Figure 4.4 shows that this observed phenomenon can explain the difference of growth kinetics between cavities in the sample.

Figure 4.4 - Inflate acceleration $\left[\frac{vx}{s^2}\right]$ vs distance from the edge $[px]$ for EPDM 1,6 - The abscissa represents the second derivative of the interpolation function and the ordinate represents the minimum distance of the cavity to the free surface.

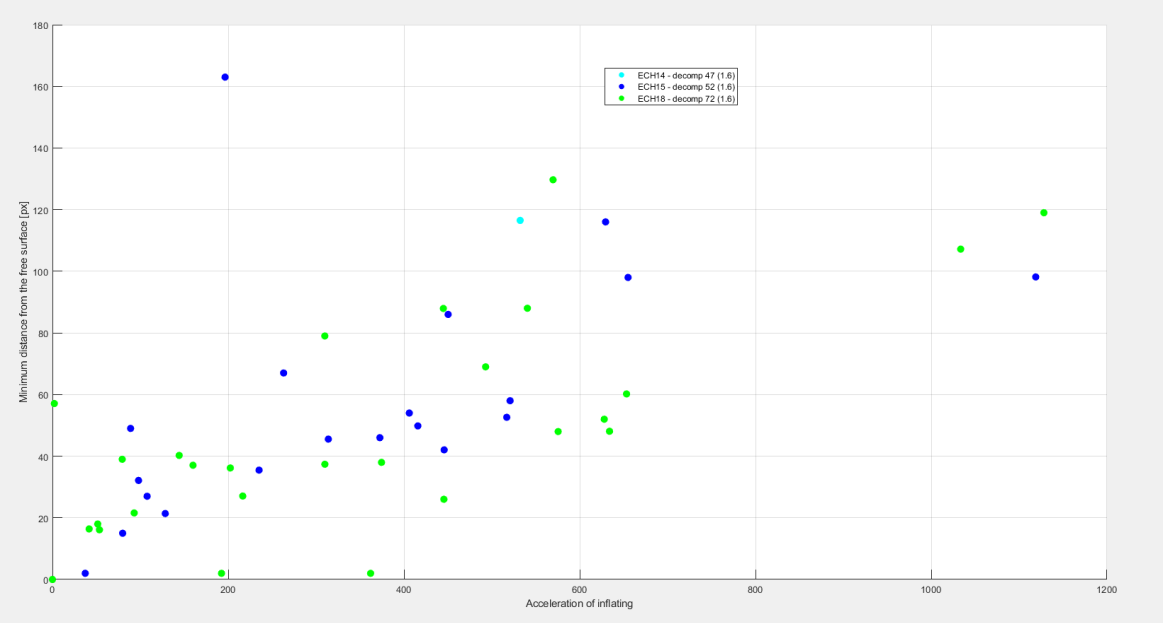

Source: Ownership by author (2022)

When analyzing the accelerations for all the EPDM with different crosslink densities, a distinct magnitude order for the accelerations was reported, as shown in Figure 4.5. It means that the distance from the free surface is not the only phenomenon working on the growth kinetics, it has other influence factors at a microscope scale.

Figure 4.5 - The abscissa represents the inflation rate $\left[\frac{vx}{s^2}\right]$ and the ordinate represents the absolute value of the deflation rate $\left[\frac{vx}{s^2}\right]$ for all EPDM's.

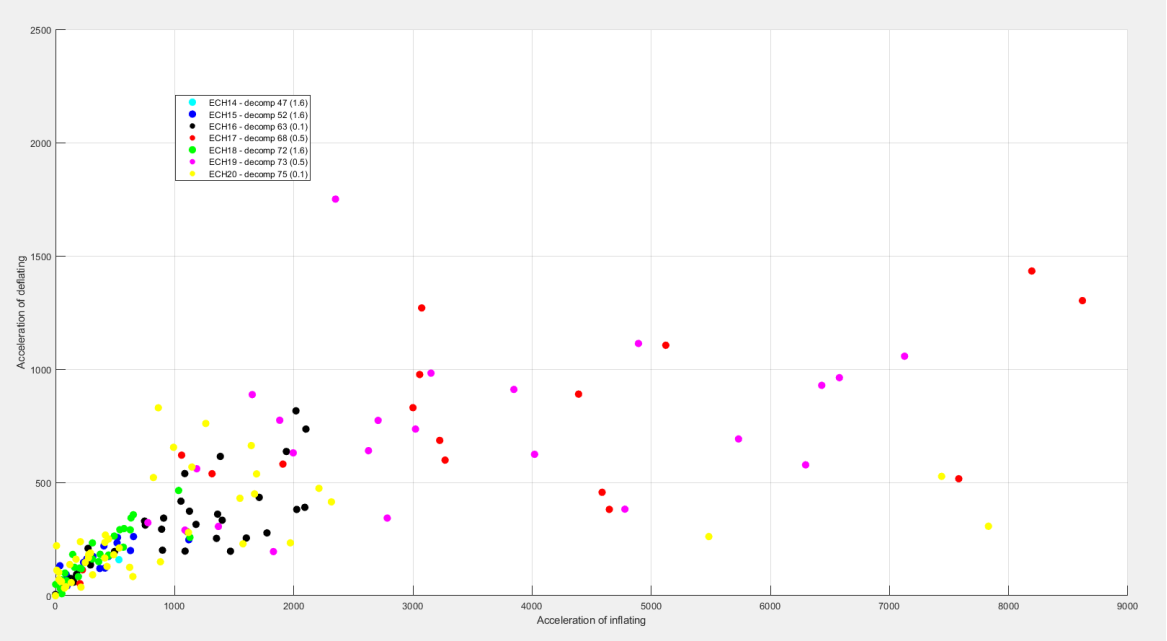

Source: Ownership by author (2022)

Moreover, for the EPDM 0,5, a big volume of cavities was observed on the sample compared withthe EPDM 1,6 and EPDM 0,1. The interesting point was that the inflate and deflate accelerations of the EPDM 0,5 were also the fattest ones. Thus, a hypothesis was made, considering that a linear relation between the maximum volume of the cavity and the inflate acceleration could exist, and consequently, with the deflate acceleration. Looking at Figure 4.6, the linear relationship is clear: fattest the inflate acceleration, largest the maximum volume of the cavity in the sample. It means that the way the cavity inflates will determine the way of deflation and even more its volume, having a direct relation betweenthe growth mechanism and the cavity's volume expansion.

Figure 4.6 – Acceleration of inflation $\left[\frac{vx}{s^2}\right]$ vs maximum volume of the cavity $[vx]$ for all the three crosslink densities.

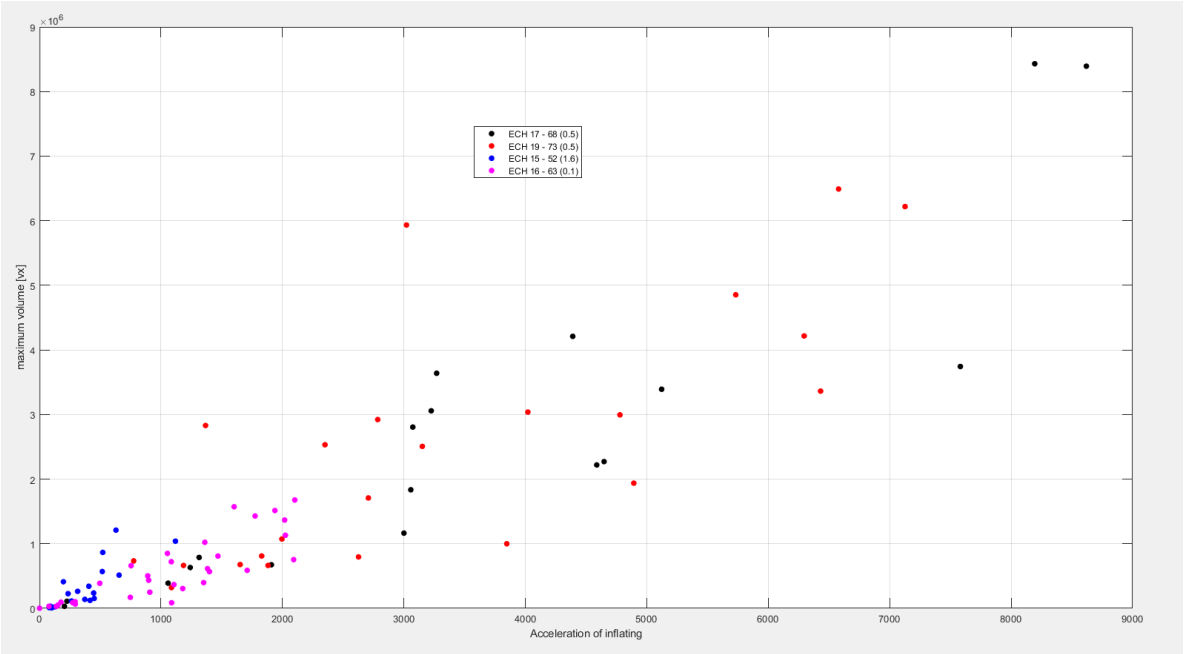

Source: Ownership by author (2022)

The sphericity, as mentioned earlier, is how spherical the cavities are. This is the most important mechanism to observe, because with it, it is possible to understand the damage process in the EPDM, also to better understand the crack formation. In other words, the decrease on the sphericity means that the cavity is not having a spherical growth with an equal expansion in all of its directions, but a preferential expansion in one direction. This direction could be the crack direction.

As mentioned before, a lot of new phenomena were observed during the internship triggering new studies. One of them was the interesting evolution of the sphericity in the first points. Even with a good resolution in time, apparently it explodes very fast until the maximum value. This creates a question about its shape at the nucleation (the beginning of the cavity life). A hypothesis was made that a low sphericity appears at the very beginning of nucleation and due to the cavity inflation, the opening of the polymer network happens, increasing its spherical shape until the maximum sphericity. This effect canbe compared to the inflation of a party balloon. After arriving to the maximum value, the sphericity starts to decrease. Besides, it was noticed that this reduction in the sphericity for the EPDM 0.5 was almost zero in comparison with the EPDM 1.6 and 0.1.

In the beginning of the study, looking at the high quantity of curves, an interesting phenomenon was detected: after the maximum, sphericity starts decreasing, as illustrated in Figure 4.7. It suggests that this point could be the beginning of the crack propagation regime, because the expansion of the cavity volume is no longer equal in all of its directions, having a preferential direction to expand.

Figure 4.7 – Example of volume and sphericity evolution for isolated cavities (ECH 20 – 75).

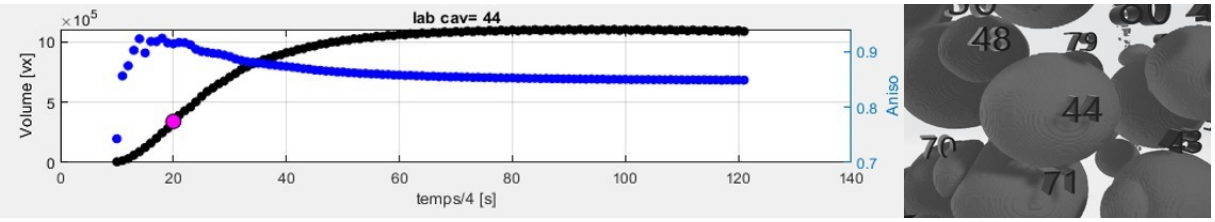

Source: Ownership by author (2022)

As already mentioned, for the EPDM 0,5 (Figure 4.2), this reduction was almost zero, suggesting that the crack propagation regime had a different mechanism or, even better, that it did not exist for those cavities.

4.2 Interaction effect between close cavities

As introduced before, cavities with intrusion of other cavities into the processed volume are named close cavities. These cavities have some particular effects that need to be discussed separately to better understand the phenomenology of the whole process. The close cavities were divided in two types: couple of cavities and a group of cavities, with the objective of analyzing if there is a different effect associated with the closeness in a couple or an amount of cavities.

4.2.1 Couple of cavities

Couple of cavities had their volume evolution unaffected by the proximity between them, having the same trend of isolated cavities. Although, the sphericity is visually affected by the vicinity between them, as shown in Figure 4.8. For isolated cavities, the

sphericity has its values varying between 0,8 -1,0, and for close cavities these values decreased to 0,6 - 0,8.

Figure 4.8 - On the top, an example of close cavities for the EPDM 0,1 (ECH 16 - 63) and at the bottom,the close cavities for the EPDM 0,5 (ECH 17 - 68).

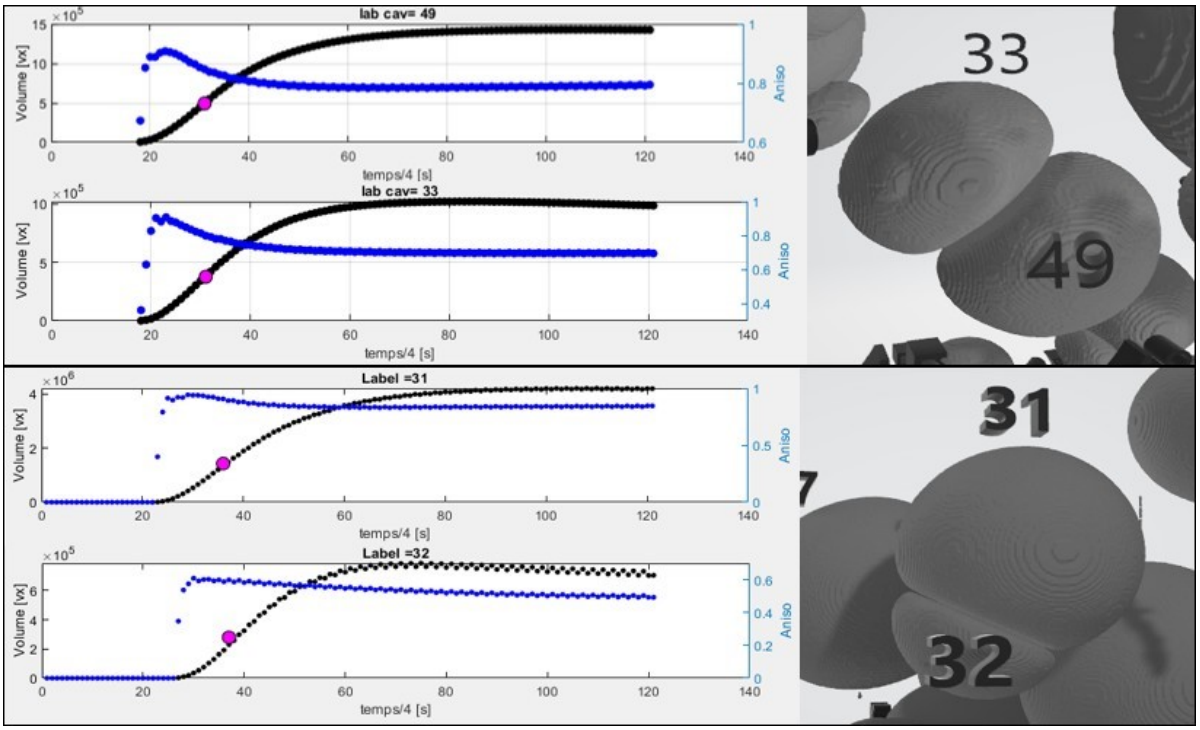

Source: Ownership by author (2022)

For all couples of cavities with different crosslink densities, the first nucleated cavity is the biggest one and its evolution remained unaffected by the second one. As well, if nucleated at almost the sametime, both cavities had almost the same maximum volume. Also, the sphericity of the cavity nucleated later was smaller than the sphericity of the first one, because the influence of the closeness for the smaller cavity is more expressive than for the bigger cavity. Furthermore, all cavities exhibited the initial spherical regime, even if they were nucleated at the same time or delayed. This means that theyhave a spherical growth and from a due point they lose this spherical growth. It happens because an external effect, the vicinity of another cavity or a detectable crack initiation.

To better understand the formation of close cavities and its effects, Table 4.1 provides some examples to compare isolated cavities with close cavities. The methodology consisted in picking one cavityof a couple and finding an isolated cavity with almost the

same size, given a reference of what should be the evolution of a cavity under this effect.

Table 4.1 - Comparison between isolated cavities and close cavities with approximated sizes.

Sample	Type of the cavity	Mean radious of the cavity for inflection point [px]	Time of the inflecti onpoint [t*4 s]	Mean radious of the max sphericity point [px]	Time of max sphericity [t*4 s]	Inflate accelerati on[vx/s^2]
ECH 15 -52	Isolated	30,8	31	30,8	31	406,04
	Close	34,6	30	24,9	24	655,02
ECH 17 -68	Isolated	53,5	32	51,2	31	3056,9
	Close	54,6	30	24,5	22	4587,9

Source: Ownership by author (2022)

It is important to highlight that all cavities in Table 4.1 had almost the same nucleation time, even for the couple of cavities. With that, the comparison could be taken into account with accuracy. In this sense, taking the same hypothesis as assumed for isolated cavities, the starting point for the detectable crack propagation regime would be when the sphericity reaches the maximum value and starts decreasing. However, under the closeness effect, the beginning of the crack formation would happen before. In other words, close cavities have an effect of mechanical constraint, changing the characteristic of crack propagation. Furthermore, the inflate coefficient for the close cavities is bigger than the one for the isolated cavities. It suggests that a cavity under a mechanical constraint, would inflate faster than the cavity without this constraint. Using the same analogy of the party balloon, when inflated against awall, for the same conditions of inflation as a normal balloon, it would inflate faster, but directionally. Besides, the cavities chosen in this comparison had the same distance to the free edge and were also under the hypothesis of having the same quantity of hydrogen passing through them, neglecting the change of gas between cavities.

4.2.2 Groups of cavities

During the campaign of analysis, another arrangement of close cavities was evaluated. This amountof cavities following a line were named "snake" cavities in this study, as shown in the Figure 4.9.

Figure 4.9 – Snake cavities for the EPDM 0,1 (ECH 16 – 63). The plots have labels in order of apparition and the red line represents the “snake”.

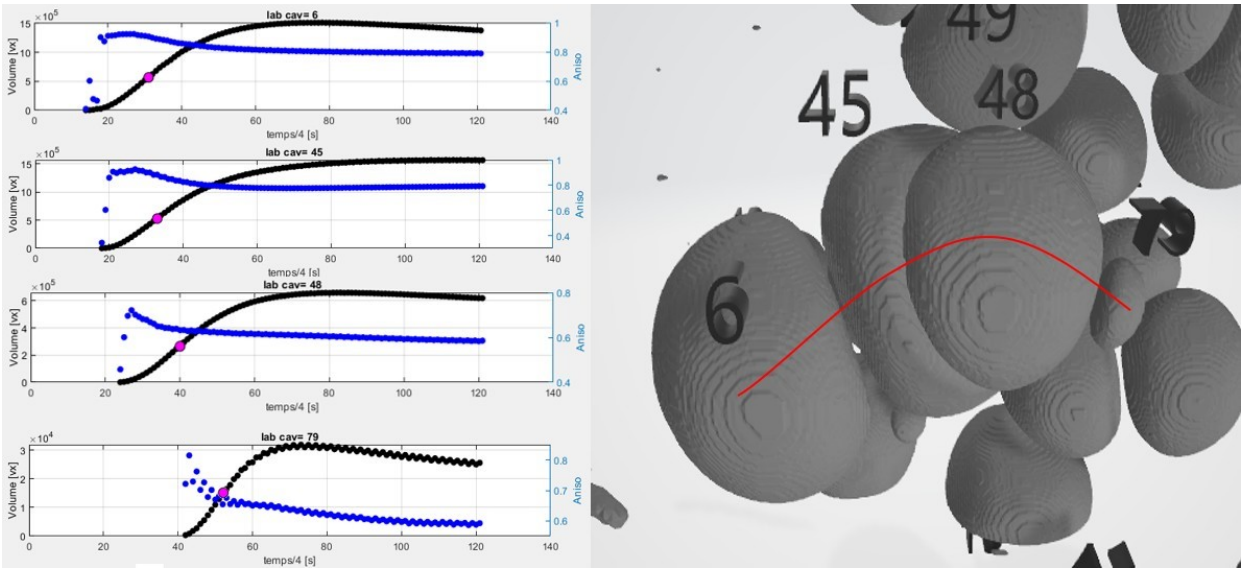

Source: Ownership by author (2022)

Looking at Figure 4.9, it is clear that the nucleation process follows a chronological order, creating a shape similar to a snake. Considering the previous results showing that cavities turn out to be anisotropic at a given stage, the question was to know if the delayed nucleation of cavities could resultfrom stress concentration ahead of the "tip" of the already existing ones. Although observed a chronological order for the particular case of Figure 4.9, for almost of the cases the nucleation was random, not following the expected order, as displayed in Figure 4.10. In conclusion, there is no privileged direction of nucleation and the chronology of the nucleation does not necessarily follow a path.

Figure 4.10 - Snake cavities for the EPDM 0,5 (ECH 19 - 73). The plots have labels in order of apparition and the red line represents the "snake".

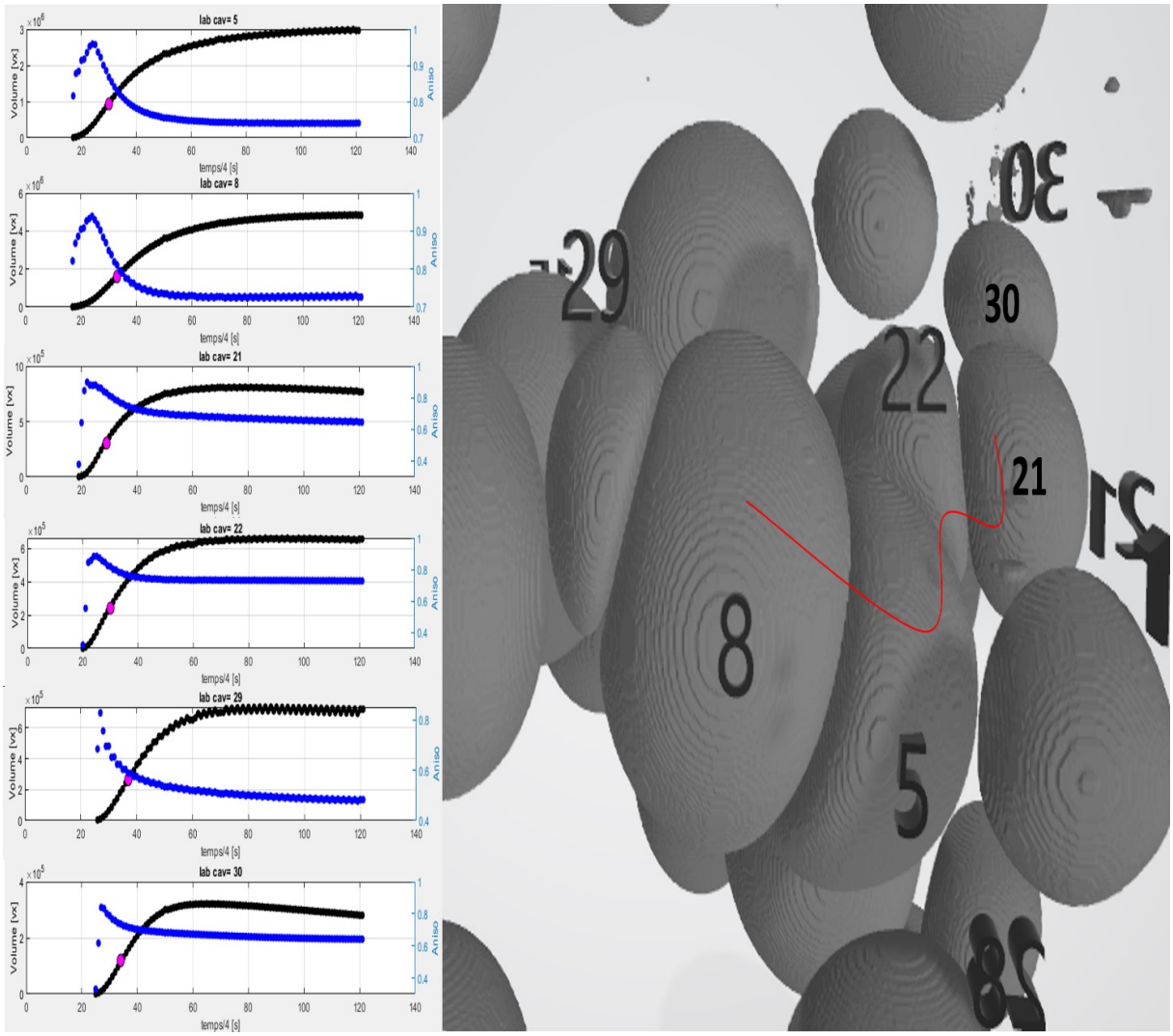

Source: Ownership by author (2022)

4.3 Damage mechanisms

The damage mechanisms is the most important part of this study. Relating it with cavitation, it would be possible to avoid failure due to this phenomenon and to increase the life time of components under this environment of decompression with hydrogen. Figure 4.11 shows the 3D reconstructionof two tomographies, the first one at the middle of the cavitation process and the second showing the residual cracks generated in the polymer after the decompression was finished.

Figure 4.11 – 3D visualisation of two tomographies (ECH 15 -52) at t_1 = 400 *s* (grey – cavitation process) and t_2 = 1000 s (red – residual damage).

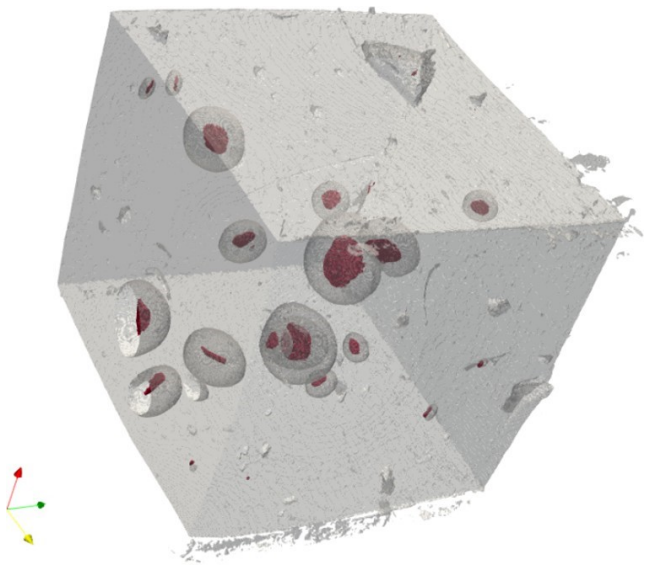

Source: Ownership by author (2022)

Looking at Figure 4.11, it is clear that cavities growth is governed by crack propagation. Furthermore, looking at Figure 4.12, the hypothesis made was that the biggest principal axis and its orientation in space could have a relation with the space orientation of the crack in the sample.

To have a temporal evolution of the principal axis direction, a methodology was created using the eigenvalues and eigenvectors of the cavity, as explained in section 6.

Then, it was possible to understand the evolution of the principal axis and correlate it with the change of the sphericity and with the crack formation. In this sense, a convergence of the principal axis angle was observed after a given time, creating a plan, as shown in the view Y versus Z of Figure 4.13.

In other words, if the principal axis converges to a preferential direction, it means that it could be the same plan of the crack. Plotting the crack over the evolution of the angles in space, the hypothesis was validated for isolated cavities, as shown in Figure 4.14. As a rule, the direction of the principal axis after its convergence is the crack's plan, which means that the study of the sphericity is relevant as an indicator of the crack propagation.

Figure 4.12 – 2D view of two tomographies (ECH 15 -52) at t_1 = 400 *s* (grey – cavitation process) and t_2 = 1000 s (red – residual damage).

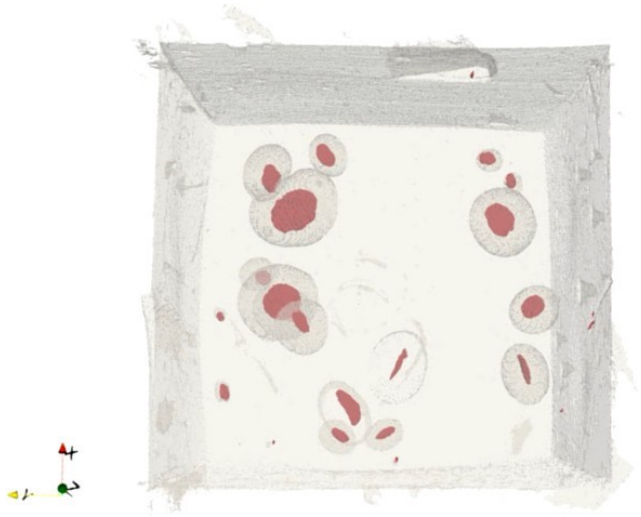

Source: Ownership by author (2022)

Figure 4.13 - Example of the directional evolution of the biggest principal axis for an isolated cavity. The norm of the vector represents the size of the principal axis and the colors, the time evolution.

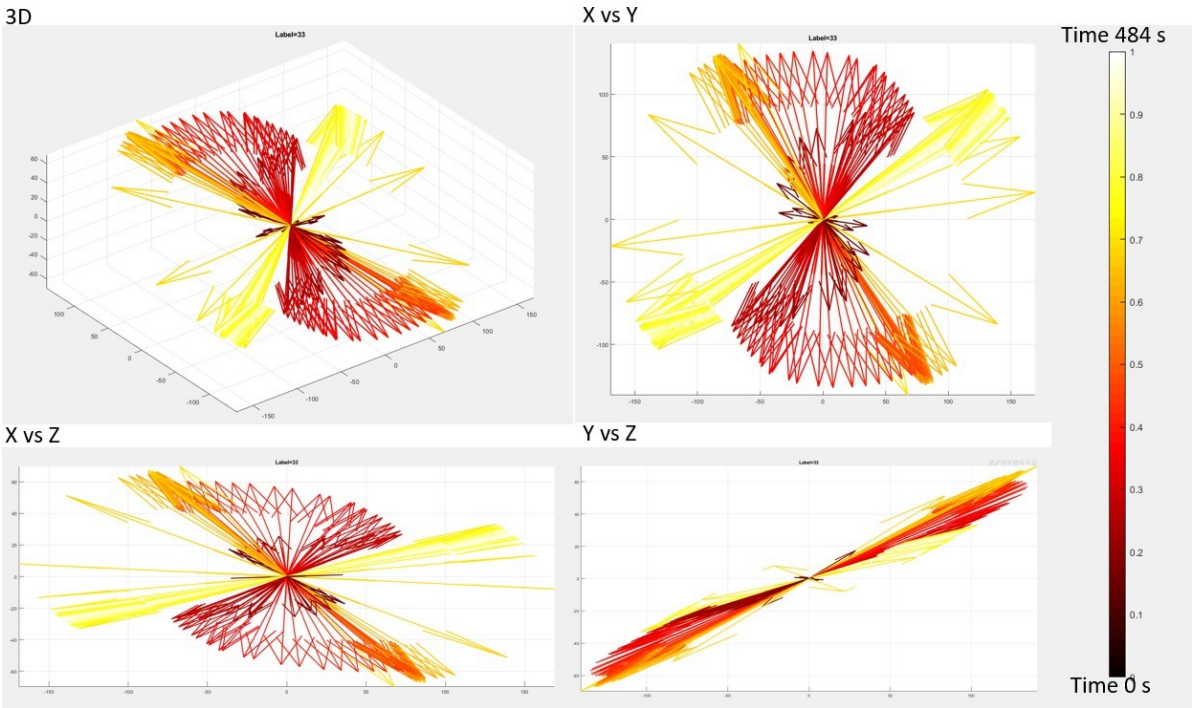

Source: Ownership by author (2022)

Figure 4.14 - Cracks in the space (blue) with the arrows of the principal axis's direction over the time.

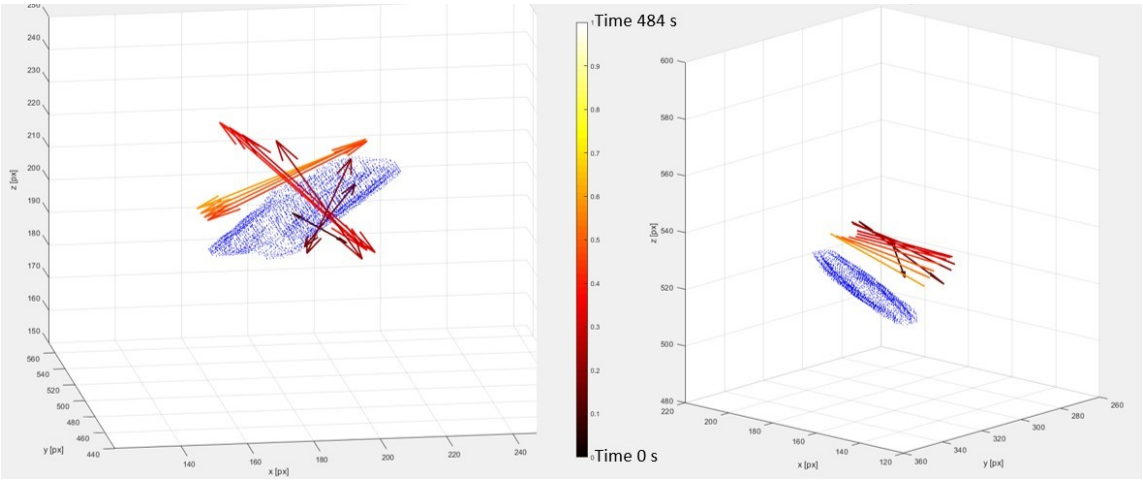

Source: Ownership by author (2022)

4.4 Global swelling of the sample

The term swelling in this study is regarding the inflation percentage of the specimen without volume of cavities. This study was the first to analyze this property, as shown in Table 4.2 and calculated as:

$$swelling = 100 * \frac{\left(Volume_{sample}\right)_{max} - \left(Volume_{sample}\right)_{min}}{\left(Volume_{sample}\right)_{min}} \quad (2)$$

A significant volume change was observed in the "matrix" of the EPDM, even without the cavities volume. This observation proves that some swelling processes, not known yet, are activated at a microscopic scale.

Table 4.2 – Values of swelling for each sample.

Crosslink density	Sample	Swelling matrix[%]
EDPM 1,6	ECH 14 – decompression 47	4.90
	ECH 14 – decompression 49	4.17
	ECH 18 – decompression 72	7.73
	ECH 15 – decompression 52	7.70
EDPM 0,5	ECH 17 – decompression 68	24.55
	ECH 19 – decompression 73	25.10
EDPM 0,1	ECH 16 – decompression 63	13.09
	ECH 20 – decompression 75	13.51
	ECH 13 – decompression 45	4.71

Source: Ownership by author (2022)

In addition, Figure 4.15 shows an example of the evolution of the volume matrix within time.

Figure 4.15 - Example of swelling for the ECH 17 - 68 - The colors represent the evolution of the number of cavities and the red line represents the initial volume of the sample before compression due to pressurization.

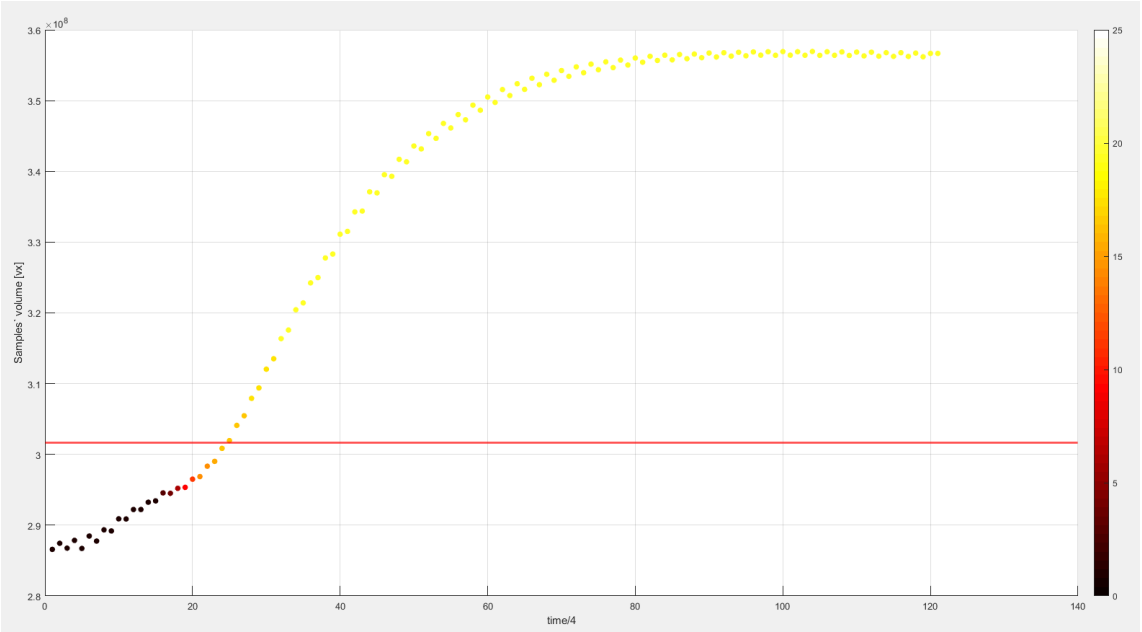

Source: Ownership by author (2022)

At the beginning of decompression, the sample had a smaller volume compared to the red line (sample volume at the ambient pressure). Then, with the beginning of the pressure release rate, the sample volume starts to increase, exceeding its volume at the ambient pressure, until its convergence.It is interesting to note that the profile of volume evolution for the sample is the same profile for the volume evolution of the cavities.

Withal, the relation between the total volume of the cavities and the sample volume was analyzed.The edge effect, described in Fazal et al. [2], was also detected in this study. To resume, the edge effect is the phenomenon of cavities close to the free surface that has a volume reduction quickly after reaching the maximum volume, as illustrated at Figure 4.17. It differs from the isolated cavities, that keep a rather constant volume. It is interesting to note that when the volume of cavities reduces, the sample volume also reduces with the same

slope as the inflation, as illustrated at Figure 4.16. In otherwords, the volume reduction rate of cavities close to the free surface is the same of the volume reduction rate of the EPDM matrix.

Figure 4.16: Evolution of the sample's volume compared to the sum of cavities's volume.

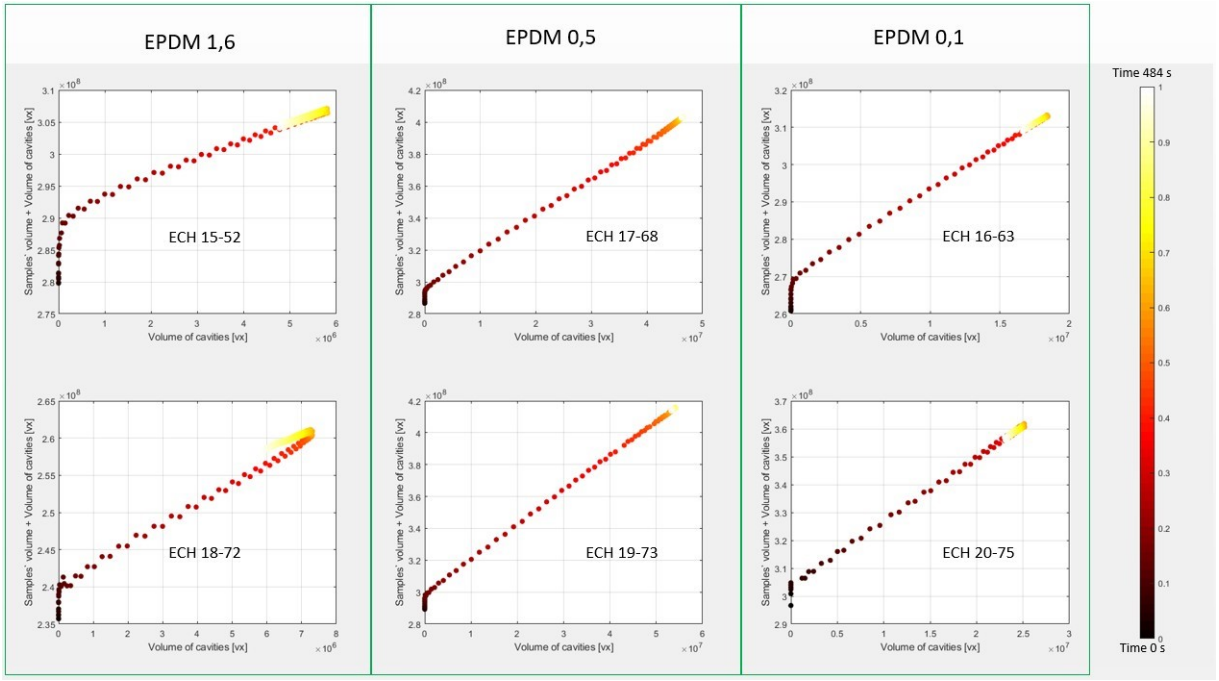

Source: Ownership by author (2022)

Finally, it was observed a hysteresis only for one specimen of the EPDM 1,6, maybe due to problems during the experiment. Looking at the second sample, such hysteresis was not observed.

Figure 4.17 – Example of a cavity under the edge effect. On the top, the 3D image with the labels of the tomography 100 ($t = 400\ s$) for the ECH 15 – 52 and at the bottom the evolution of the volume and sphericity over time.

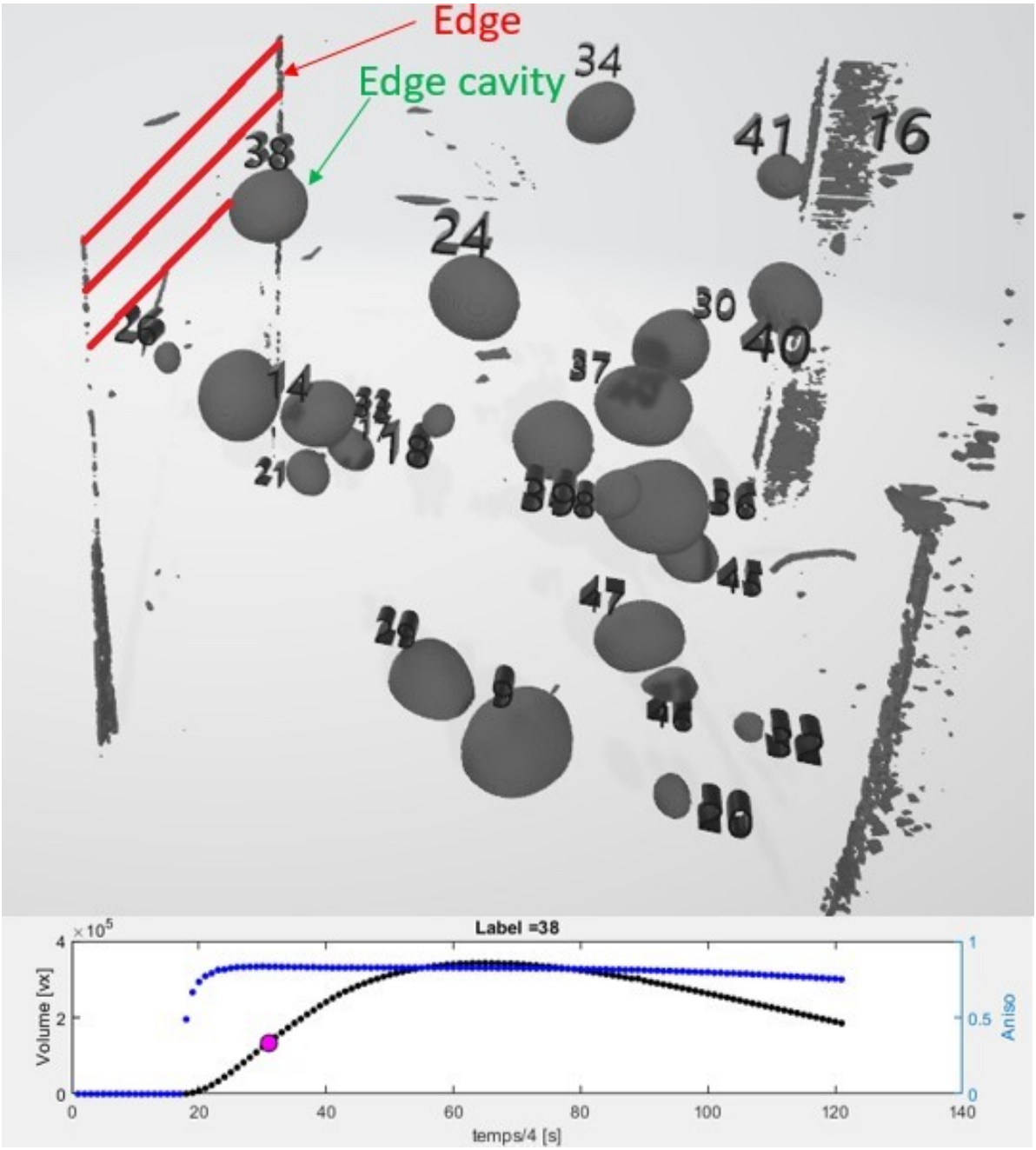

Source: Ownership by author (2022)

5. Conclusion and future works

This work aimed to better understanding the phenomena of cavities in polymers exposed to a decompression with hydrogen, but with a better resolution in time and space, due to the Synchrotron SOLEIL. Effects could be captured and discussed for the first time within the goal of understanding the kinetics growth of the phenomena related with the damage process. The kinetics of close cavities was studied with a much better accuracy, confirming some observations made in the latest works. Lastly, the effects of different crosslink density of EPDM were considered, even not being so evident during the discussions, they were present all the time. In this sense, the conclusions were provided:

- The acceleration of inflate and deflate are correlated, validating the previous approximation;
- Isolated cavities far from the free surface have bigger growth accelerations, not meaning that the distance to the free surface is the only influence factor. Furthermore, different orders of magnitude from EPDM's of different crosslink densities were demonstrated, meaning that exists a microscopic influence in the kinetics;
- There is not enough evidences to prove that the low sphericity in the beginning of the cavity life is due to the opening of the polymer network. Even better, the spatial resolution is still too coarse;
- Isolated cavities have the plan of convergence of the principal axis coincident with the same plan of the crack;
- The EPDM 0.5 has the bigger growth accelerations, consequently the biggest volume of cavities;
- – For close cavities, the growth accelerations are bigger compared to isolated cavities;
  - – There is no other cooperativeness between cavities than an adaptation shape, seeing each other as a mechanical constraint;
- Snake cavities are just an amount of coupling of cavities, not representing a

different phenomenon;

- More experiments must to be conducted to make conclusions about the hysteresis observed on the sample;
- The study strongly suggests that the scale of study chosen is not the one that could explain all the phenomena, there is a microscopic influence that should be taken into account.

For future work, it will be necessary to improve the statistical data of the phenomena for all the EPDM studied, using a better range of crosslink density, aiming to understand better the microscopic influence.

6. References

CASTAGNET, Sylvie; MELLIER, David; NAIT-ALI, Azdine; BENOIT, Guillaume. “In-situ x-ray computed to- mography of decompression failure in a rubber exposed to high-pressure gas”. In.: *Polymer Testing*, v. 70, 2018. Disponível em: <https://www.sciencedirect.com/science/article/abs/pii/S0142941818309310?via%3Dihub>.

FAZAL, Mahak; CASTAGNET, Sylvie; NAIT-ALI, Azdine; NISHIMURA, Shin. “ Local kinetics of cavitation in hydrogen-exposed epdm using in-situ x-ray tomography: Focus on free surface effect and cavityinteraction”. In.: *Polymer Testing*, v. 91, 2020. Disponível em: <https://www.sciencedirect.com/science/article/abs/pii/S0142941820306097>

A - Appendix

A.1. Interpolation

The interpolations in this study were made with an application of a Matlab function to fit curves,named **Curve Fitting**. The properties used were:

```
fitOptions =

    Normalize: 'off'
      Exclude: []
      Weights: []
       Method: 'LinearLeastSquares'
       Robust: 'Off'
        Lower: inf
        Upper: inf
```

The definitions are:

- 'Normalize' — Option to center and scale data;
- 'Exclude' — Points to exclude from fit;
- 'Weights' — Weights for fit;
- 'Method' — Fitting method;
- 'Robust' — Robust linear least-squares fitting method;
- 'Lower' — Lower bounds on coefficients to be fitted;
- 'Upper' — Upper bounds on coefficients to be fitted.

A code was created to interpolate and stock the coefficients. To verify the results, all the interpolations done for all cavities were plotted, looking at the inflate and deflate curves, beside the verification of the inflection point with the plot of the gradient over all the growth curve, as illustrated in Figure A.1.

Figure A.1 – Example of the plots to verify the interpolation done.

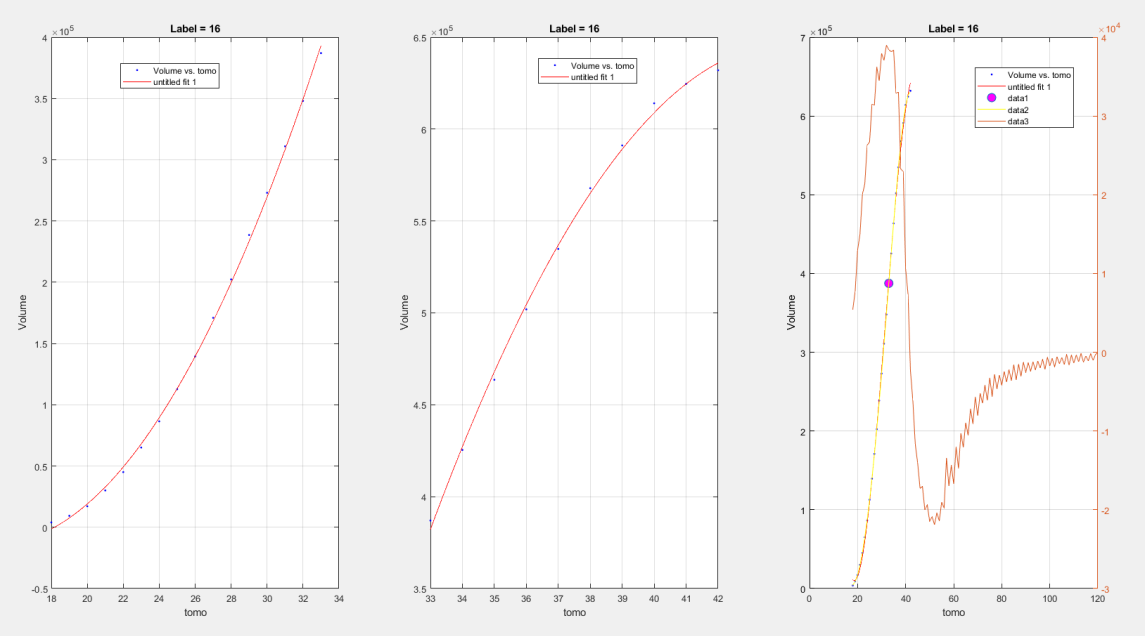

Source: Ownership by author (2022)

Directional Evolution

In order to create the directional evolution, the Eigenvalues and the Eigenvectors provided by the function **regionsprops3** were used. Briefly, each cavity has a representative ellipsoid with the same second central moments. With this 3x3 matrix of the second central moments, its Eigenvalues and respective Eigenvectors were calculated, giving the direction and the modulus of the principal axis. This direction given is a normalized vector referenced in the centroid of the cavity. All this descriptionis the theory of the **regionprops3** to find these values. Thus, with these vectors and their size, it was possible to understand the evolution of the biggest principal axis over the time.